Geothermal Energy

RESEARCH Open Access

Geo-temperature response to reinjection in sandstone geothermal reservoirs

Jialong Li[1], Fengxin Kang[1,2,4*], Tong Bai[3], Zhenhan Li[1], Qiang Zhao[1], Pingping Zhang[3], Tingting Zheng[5] and Haibo Sui[5]

*Correspondence:
kangfengxin@126.com

[1] School of Water Conservancy and Environment, University of Jinan, Jinan 250022, China
[2] Shandong Provincial Bureau of Geology & Mineral Resources (SPBGM), Jinan City, China
[3] Shandong Provincial Bureau of Geology and Mineral Resources (SPBGM), No. 2 Institute of Hydrogeological and Engineering Geology, Dezhou City, China
[4] College of Earth Science and Engineering, Shandong University of Science and Technology, Qingdao 266590, China
[5] Shandong Provincial Bureau of Geology and Mineral Resources (SPBGM), 801 Institute of Hydrogeology and Engineering Geology, Jinan, China

Abstract

To study the evolution rules and behaviors of heat transport in a sandstone geothermal reservoir caused by cooled water reinjection, this research focuses on the quantitative relationship among reinjection parameters and the thermal breakthrough time of production wells. The permeation, tracer, and reinjection tests were conducted in a simulation model using a large sand tank in conjunction with the numerical simulation method based on COMSOL Multiphysics. Subsequently, sensitivity analysis and nonlinear fitting were performed to investigate the effects of fluid viscosity and density on the reinjection process, and to analyze the impact of reinjection parameters on the thermal breakthrough time of production wells, along with their underlying mechanisms and law. The results indicate that the migration velocity of reinjection water is greater in coarse sand layer compared to that in medium sand layer, and the thermal breakthrough time t is linearly correlated with reinjection rate (Q) raised to the power of − 0.85, temperature difference (ΔT) raised to the power of − 0.21, and spacing between the production and reinjection wells (R) raised to the power of 1.4. The correlation equation and analysis show that when the temperature difference between production and reinjection ΔT is more than 30 ℃, the influence of ΔT on the thermal breakthrough time of production well becomes weak, because ΔT exerts an effect on the thermal breakthrough time of production well t by influencing the relative position of the 18.5 ℃ isotherm in the temperature transition region. The error in reinjecting high-temperature fluid into low-temperature fluid may be corrected by introducing a viscosity correction coefficient α_{μ}.

Keywords: Reinjection parameters, Simulation test, Numerical simulation, Geo-temperature, Mechanism of evolution

Introduction

Geothermal energy is thermal energy inside the earth that can be used economically by human beings (Rybach et al. 1999; Sanyal 2005; Kang et al. 2013). Low-temperature hydrothermal resources are a relatively green and low-carbon form of clean energy, widely distributed within the deep-seated sandstone and karst-developed formations of sedimentary basins (Kang 2013; Tomasini-Montenegro et al. 2017; Sullivan and Mannington 2005). In recent years, there has been a noticeable escalation in energy utilization, accompanied by a concurrent exacerbation of associated environmental issues

(Santoyo et al. 2018; Wang et al. 2008; Chen et al. 1985; Gao et al. 2009). Thus, geothermal energy has gradually attracted the attention of researchers and an upsurge in geothermal development has occurred (Wright 1995; Axelsson et al. 2001, 2002). However, large-scale exploitation of deep geothermal water would cause a decrease in the heat reservoir pressure and the utilization rate of geothermal resources (Axelsson et al. 2004, 2005; Rybach et al. 2003). The direct discharge of tail water can also cause serious waste of water resources and thermal and hydrochemical pollution of the surrounding environment (Wu et al. 2016; Kang et al. 2011; Zhao 2013). Geothermal reinjection plays an important role in improving the utilization rate of geothermal resources, reducing tail water discharge, maintaining the geothermal reservoirs pressure, and realizing the sustainable utilization of geothermal resources (He and Liu 2003; Zhu et al. 2012; Hjuler et al. 2019). However, reinjection will inevitably lead to a decrease in the reservoir temperature because the temperature of the geothermal tail water reinjection is much lower than the reservoir temperature. When the cold-front surface of the reinjection tail water migrates to the production well, it causes a thermal breakthrough of the production well. As the water temperature in the well decreases, the utilization rate of the geothermal resources also decreases rapidly, until the exploitation value is lost (Obembe et al. 2016; Seibt and Kellner 2003). Therefore, it is of great significance to study the evolution of the geo-temperature of reservoirs caused by geothermal tail water reinjection (Weibel et al. 2017; McCreesh et al. 1991; Cade et al. 1994).

Regarding this problem, Lei and Zhu (2010) used a mathematical model combined with a numerical simulation method to study the influence of the rate of reinjection on the temperature and pressure field of a thermal reservoir. Liu et al. (2019) monitored the temperature, temperature gradient, and geothermal warming rate of an entire well section, qualitatively analyzed and quantitatively calculated the sources of the thermal reservoir temperature recovery in a geothermal reinjection well in a sandstone thermal reservoir, and found that the main sources of heat were heat conduction and geothermal water flow from the relatively high-temperature strata in the peripheral area. Bodvarsson (1972) and Dutton and Loucks (2010) calculated the thermal pollution range caused by cold water reinjection in a homogeneous isotropic porous media through theoretical analysis and determined the relationship between the thermal pollution range and the aquifer thickness, rate of reinjection, and reservoir heat capacity. Sayantan and Ganguly (2014) and Stefansson (2000) proposed an analytical solution to describe the transient temperature distribution of a geothermal reservoir when cold water is injected, and studied the influence of different reinjection rates, thermal conductivities, and porosities of porous media on the transient heat transfer phenomenon. The results showed that the reinjection rate and thermal conductivity have important effects on the transient temperature distribution. Saeid et al. (2014), Qiu (2017) and Megel and Rybach (2000) combined numerical and experimental methods to study the effects of fluid density and viscosity on heat flow in saturated porous media and found that considering the characteristics of fluid density and viscosity variations with temperature is crucial in predicting the thermal breakthrough time of production well. Sippel (2013) established a thermal reservoir model of the southwest region of the Hague using numerical simulation methods, and they studied the influences of the reservoir structure, porosity, and permeability on the thermal breakthrough of a thermal reservoir production well. Franco (2014),

Sauty (1980), and Bedre (2012) qualitatively investigated the importance of the flow rate, the spacing between the production and reinjection wells, the reinjection temperature, and the reservoir geometry in the lifetime of the geothermal system. Their results are only suitable for preliminary design and use by geothermal engineers in the early stages of a project. The mentioned above factors affecting the thermal breakthrough time of production well have been extensively studied, but large model tests and human-adjustable parameters of geothermal production and reinjection system have not been comprehensively studied and analyzed. Ayling et al. (2016) conducted two inter-well tracer tests, and storage capacity relationships for the Habanero reservoir indicate that the reservoir is moderately heterogeneous, and has both fast and slow flow pathways within it. Guerrero et al. (2023) proposed an updated conceptual model of the Las Tres Virgenes hydrothermal system, incorporating geochemical and geophysical evidence. The proposed model revealed that storativity and permeability of the faults have a great influence on the long-term sustainability of the system.

In this study, the evolution of the internal temperature field of a thermal storage model due to heated reinjection was studied using a simulation test model of a large sand tank experiment. Then, based on the results of permeation tests and tracer tests using the sand tank simulation test model, the equivalent numerical model of the sand tank simulation test model was established. Hydrodynamic parameters of the numerical model were also calibrated, and the established equivalent sand tank numerical model was used to study the quantitative relationships between three reinjection parameters (the reinjection temperature, rate of reinjection, and spacing between the production and reinjection wells) and the thermal breakthrough time of the production well.

Research methodology

Experimental study of sand tank simulation test model

Design of sand tank simulation test model

(1) Main structure of sand tank simulation model

The sand tank simulation test model was 12 m long, 6 m wide, and 6 m high, and the thermal reservoir medium was well-sorted and rounded quartz sand, which was cleaned and then backfilled in layers using a vibrating flat plate. Every 30 cm was a layer with uniform vibration. During the backfilling, sand compaction samples were collected for compactness tests. The bottom 4–6 m interval was coarse sand; the 2.8–4 m interval was medium sand; and the upper layer (0–2.8 m) was backfilled clay, which served as a water barrier (Fig. 1).

(2) Design of borehole in sand tank simulation test model

The sand tank simulation test model was equipped with one production well, one reinjection well (Fig. 2), two backup reinjection wells, and 13 water level monitoring holes (Fig. 3). The production and reinjection wells were located at the two lateral ends of the sand tank, 1 m away from the lateral sides of the sand tank, on the lateral central axis of the sand tank, and 3 m away from both sides of the sand tank. The two backup reinjection wells were symmetrically distributed along the horizontal central axis of the reinjection wells and were 1.5 m away from the horizontal

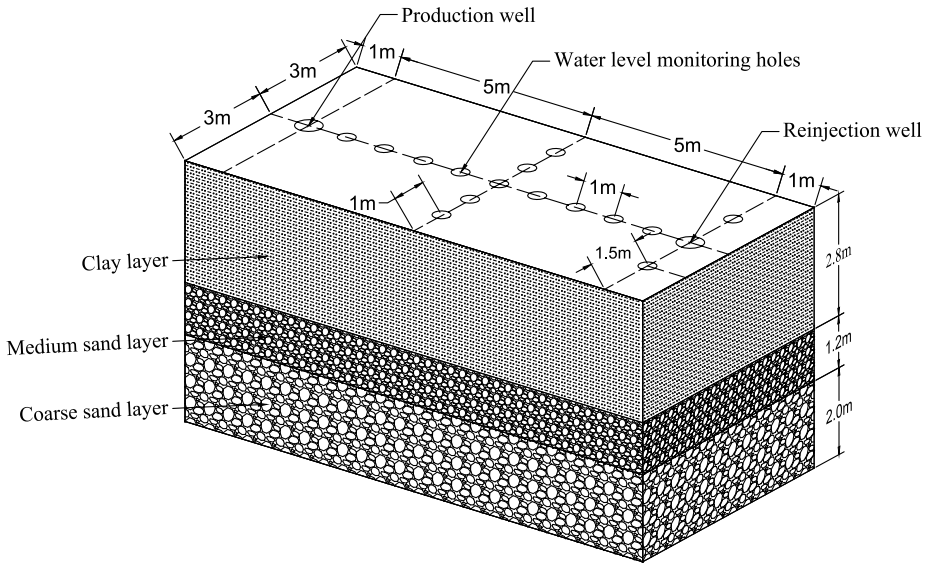

Fig. 1 Schematic diagram of the sand tank simulation test model

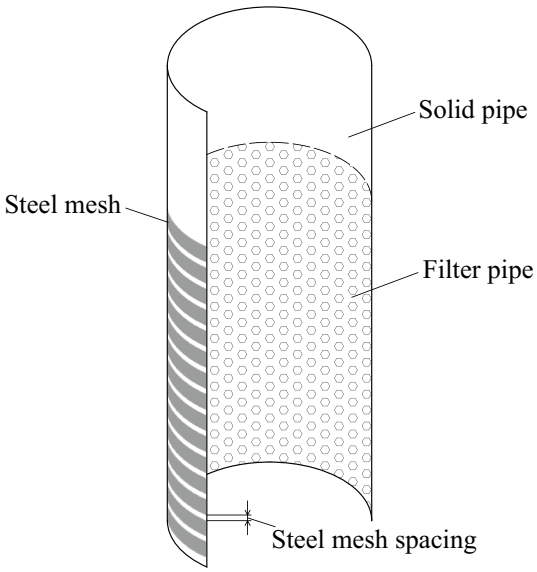

Fig. 2 Filter pipe structure diagram of reinjection well

long side. The details of the well distribution are shown in Fig. 4, and the specific well pipe size parameters are presented in Table 1.

(3) Sand tank monitoring point design

Water level monitoring probes were installed in the production well, reinjection wells, and water level monitoring holes to collect real-time water level data. Electromagnetic flowmeters were installed in the production well and reinjection wells to collect real-time data on the production and rate of reinjection. The arrangement of the temperature and pressure monitoring points inside the sand tank is shown in Figs. 5 and 6. A total of five monitoring surfaces were laid out perpendicular to the *X*-axis direction with an interval of 3 m. These surfaces are labeled a–e; a total of

Fig. 3 Water level monitoring hole

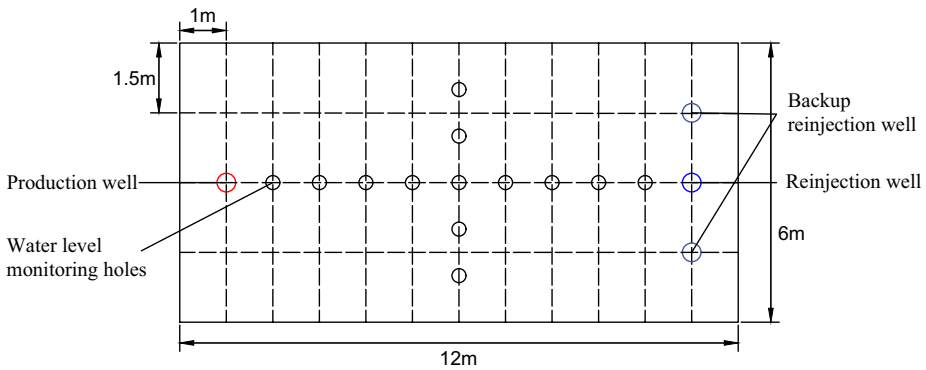

Fig. 4 Top view of the sand tank simulation test model

Table 1 Structural parameters of production and reinjection wells and water level monitoring holes

Well type	Borehole diameter (mm)	Borehole wall diameter (mm)	Gravel thickness (mm)	Diameter of filter pipe (mm)	Steel mesh spacing of water filter pipe (mm)
Production well	100	–	–	10	0.5–1.0
Injection well	220	88	66	10	0.5–1.0
Water level monitoring holes	70	–	–	5	–

four monitoring surfaces were laid out perpendicular to the *Y*-axis direction with an interval of 2 m. These surfaces were labeled A–D. A total of four monitoring surfaces were laid out perpendicular to the Z-axis direction with an interval of 1 m. These surfaces were labeled 1–4. The pressure and temperature monitoring points were located at the intersection of all of the surfaces for real-time temperature and pressure data collection. The locations of the water sample sampling points were the same as the location of the temperature and pressure monitoring points inside the sand tank, but the number was halved and arranged at intervals.

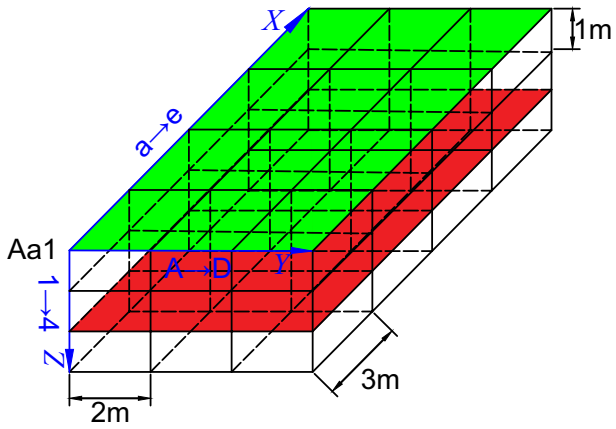

Fig. 5 Temperature and pressure monitoring points and labels

Model test

The sand tank was injected at a slow and stable rate, with a flow rate of ~ 5 m^3/h. While injecting the water, the water level in the monitoring holes and the changes in the readings of flowmeters in the production and reinjection wells, the water level sensors, and the pressure and temperature sensors inside the sand tank were closely monitored, and the commissioning of the monitoring equipment was carried out. The model test was carried out after the geothermal water filled the entire thermal reservoir medium, the water surface in each piezometric tube remained flush, and the pressure and temperature in each layer were stabilized. At this time, the head of the sand tank simulation test model was 5.2 m (with the bottom of the sand tank defined as 0 m) and the temperature was 15 °C.

(1) Permeation tests

After the completion of the pre-test preparation, the permeation tests of the model were carried out first, and the testing was divided into three stages, i.e., large depth

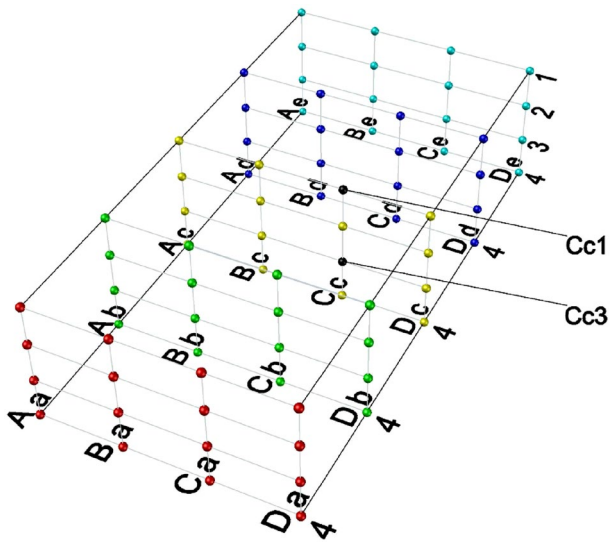

Fig. 6 Water sample sampling points and labels

reduction, medium depth reduction, and small depth reduction. The rate of water production is the same as the reinjection rate, and the production and reinjection process is carried out simultaneously. The reinjection rate of the three drawdowns are 1.10 m^3/h, 0.72 m^3/h, and 0.52 m^3/h, respectively. It needs to continue for 8 h after the water level reaches a stable level, and the three drawdown tests lasted for 6 days in total.

(2) Reinjection tests

After the reinjection tests ended and the water surface in each piezometric tube was flush again, the reinjection tests with different reinjection temperatures of the model were carried out. Since the ambient temperature of the sand tank model is low, a large amount of heat will be lost at the boundary of the model when the sand tank has high initial temperature. Therefore, the temperature of the sand tank is kept close to the ambient temperature of the external environment 15 °C, and high-temperature water is used for reinjection to reduce heat loss. First, a heating reinjection experiment was carried out at a reinjection temperature of 40 °C and a reinjection and production flow rate of 0.3 m^3/h for 14 days. After the experiment, when the sand tank temperature dropped to 15 °C, the heating reinjection experiment was continued at a reinjection temperature of 60 °C and a reinjection and production flow rate of 0.8 m^3/h for 7 days.

(3) Tracer tests

After the heating reinjection tests ended and the water surface in each piezometric tube was flush again, the tracer tests were carried out. Ammonium molybdate was selected as the tracer for the tracer tests. The reinjection and production flow rate are fixed at 0.4 m^3/h and the process of production and reinjection is carried out synchronously until the dynamic stability of the water level in the sand tank simulation test model. Then, 500 g of ammonium molybdate was dissolved in 3 L of water and the solution was instantaneously placed in the reinjection well. The frequency of water sampling for testing after reinjection is once every 4 h, and after the tracer arrives, the frequency is increased to once every 2 h. The tracer tests last for a total of 6 days.

Numerical simulation

The conceptual model of the sand tank simulation test model was established according to the actual structure of the sand tank with the same wells, sand layers and boundaries. The hydrodynamic and thermal physical parameters of the numerical model were fitted according to the experimental data from the reinjection and tracer tests conducted in the actual sand tank model. Furthermore, the study makes the following assumptions regarding the numerical model: (1) the sand layers within the sand tank model are assumed to be homogeneous and isotropic porous media with uniform properties. (2) The thermal and dynamic equilibrium between water and the porous media skeleton is considered to be instantly achieved. (3) Natural convection resulting from the density difference between cold and hot water is taken into account. Using the established equivalent sand tank numerical model, the response process and mechanism of the sandstone thermal reservoir geo-temperature to the reinjection parameters were studied.

Numerical modeling of equivalent sand tank

The COMSOL Multiphysics numerical simulation software was employed to construct a numerical simulation model that incorporates the coupling of water, thermal, and chemical processes. The model was specifically applied to simulate the dynamic changes in reservoir temperature, water level, and tracer concentration within a sand tank experimental setup. This simulation was conducted under the conditions of well production and reinjection, providing insights into the temporal and spatial variations occurring within the system. The COMSOL Multiphysics is a powerful finite element analysis tool that offers a wide range of capabilities for modeling and solving complex multiphysics problems (Liu et al. 2020). Regarding the modeling of transport in porous media, COMSOL Multiphysics provides robust features and functionalities. It offers various physics interfaces and predefined module libraries specifically designed for porous media applications. These include interfaces for fluid flow, heat transfer, species transport, and chemical reactions in porous media. However, COMSOL Multiphysics also has certain limitations. These may include computational requirements, simulation time, and specific assumptions or simplifications made in the modeling process.

1. Seepage in porous media

   In the case of a thermal reservoir aquifer, assuming the aquifer is fully saturated, the saturated pressure flow can be described by Darcy's law:

   $$\boldsymbol{u} = -\frac{K}{\rho_f g}(\nabla p + \rho_f g \nabla z), \tag{1}$$

   where $\boldsymbol{u}$ is the Darcy flow rate (m/s); K is the permeability coefficient of the thermal reservoir (m/s); p is the fluid pressure (Pa); and z is the ordinate (m).

   The fluid continuity equation can be expressed as follows:

   $$\frac{\partial}{\partial t}(\rho\phi) + \nabla \cdot (\rho \boldsymbol{u}) = Q_{\mathrm{m}}, \tag{2}$$

   where ϕ is the porosity of the porous media, and Q_{m} is the mass source term (kg/(m^3 s)).
2. Heat transfer in porous media.
   The seepage and heat transfer process in a thermal reservoir can be described by the porous medium heat transfer equation:

   $$(\rho C_p)_{\mathrm{eff}} \frac{\partial T}{\partial t} + \rho_f C_{\mathrm{pf}} \boldsymbol{u} \cdot \nabla T = \nabla \cdot (k_{\mathrm{eff}} \nabla T), \tag{3}$$

   where $(\rho C_p)_{\mathrm{eff}}$ is the effective volume heat capacity at constant pressure. For porous media, it can be expressed as follows:

   $$(\rho C_p)_{\mathrm{eff}} = \theta_{\mathrm{s}} \rho_{\mathrm{s}} C_{\mathrm{p,s}} + \theta_{\mathrm{f}} \rho_{\mathrm{f}} C_{\mathrm{p,f}}, \tag{4}$$

where θ_s is the volume fraction of the solid material, and θ_f is the volume fraction of the liquid.

The effective thermal conductivity of a porous medium k_{eff} is related to the thermal conductivity of the solid material k_s and the thermal conductivity of the fluid material k_f, and it can be expressed as the weighted arithmetic mean of the sum:

$$k_{eff} = \theta_s k_s + \theta_f k_f, \tag{5}$$

3. Solute transport in porous media.
Assuming the aquifer is fully saturated, the seepage and solute transport process in a thermal reservoir can be described by the porous medium solute transport equation:

$$\frac{\partial}{\partial t}(c_i \phi) + \boldsymbol{u} \cdot \nabla c_i = -\nabla \cdot J_i + S_i, \tag{6}$$

where c_i is the solute concentration (kg/m^3); S_i is source–sink contribution (mol/(m^3 s); J_i is the diffusion flux (kg/(m^2 s)), and can be expressed as follows:

$$J_i = -\left(D_{D,i} + D_{e,i}\right)\nabla c_i, \tag{7}$$

where $D_{D,i}$ is the dispersion coefficient (m^2/s); $D_{e,i}$ is the effective diffusion coefficient (m^2/s).

The numerical model parameters were set according to the geometric characteristics of the actual sand tank simulation test model, the vertical distribution of the aquifer media, and the location and parameters of the production and reinjection wells. The boundary conditions of the hydrodynamic, temperature, and chemical fields were the impermeable, adiabatic, and impermeable boundaries, respectively. The initial head, initial temperature, and initial concentration of ammonium molybdate were 5.2 m, 15 °C, and 0, respectively. The permeability of the sand tank numerical simulation model was inverted according to the relationships between the water level and flow rate of the production and reinjection wells in the reinjection tests and the variation in the ammonium molybdate concentration in the tracer tests. The thermal conductivity of the porous media in the sand tank model was inversely evolved according to the temperature change trend of the monitoring points in the heating reinjection tests.

Study of the effects of reinjection parameters on the temperature field of thermal reservoir

The thermal breakthrough time of the production well was used to characterize the changes in the thermal storage temperature field, and a 2 °C variation in the production temperature was set as the occurrence of thermal breakthrough. The effects of three reinjection parameters, that is, the reinjection temperature, reinjection rate, and spacing between the production and reinjection well, on the thermal breakthrough time of the production well were studied, and parameter sensitivity analysis was performed.

1. Relationships between reinjection parameters and water temperature variation in production well

Table 2 Values of reinjection parameters in sensitivity analysis

	Reinjection temperature (°C)	Reinjection rate (m^3/h)	Spacing between production and reinjection wells (m)
Condition 1	30, 40, 50, 60	0.5	10
Condition 2	30	0.5, 1, 1.5, 2	10
Condition 3	30	0.5	4, 6, 8, 10

The values of the reinjection parameters are listed in Table 2. Working conditions 1, 2, and 3 correspond to the effects of the three parameters (i.e., the reinjection temperature, reinjection rate, and spacing between the production and reinjection well) on the variations in the water temperature in the production well. The temperature variations in the production well with time under the effects of the different reinjection parameters were calculated.

2. Relationships between reinjection temperature, reinjection rate, and production well thermal breakthrough time

   The flow rate of the production well was set to 0.1 m^3/h, 0.2 m^3/h…, 0.5 m^3/h, 0.75 m^3/h…, 1.5 m^3/h, 2 m^3/h, 2.5 m^3/h, and 3m^3/h in order, and the reinjection temperature was set to 25 °C, 30 °C…, and 60 °C, respectively. Then, the thermal breakthrough time of the production well was calculated, and the relationships between the reinjection temperature, reinjection rate, and thermal breakthrough time were fitted.

3. Relationships between production and reinjection well spacing, reinjection rate, and production well thermal breakthrough time

   According to the reinjection temperature in the operation of an actual production and reinjection system, the reinjection temperature difference is usually around 30 °C. Accordingly, the reinjection temperature was set to 45 °C to study the relationships between the spacing between the production and reinjection wells, the reinjection rate, and the thermal breakthrough time. The spacing between the production and reinjection wells was set to 3 m, 4 m… and 10 m, and the time required for a thermal breakthrough of the production well for different reinjection rates was calculated. Then, the relationships between the spacing between the production and reinjection wells, the reinjection rate, and the thermal breakthrough time were fitted.

4. Parameter sensitivity analysis

   Different values of the three reinjection parameters, namely, the reinjection temperature, reinjection rate, and spacing between the production and reinjection wells, had different effects on the thermal breakthrough time of the production well. Therefore, sensitivity analysis was conducted to investigate the effects of the three reinjection parameters on the thermal breakthrough time of the production well. Sensitivity analysis was conducted using a fixed variable approach. For instance, when studying the influence of reinjection rate on thermal breakthrough time of production wells, the reinjection temperature and spacing between the production and reinjection wells were kept constant. By artificially adjusting the reinjection rate within certain fluctuations, the response of thermal breakthrough time of the production wells to this input parameter was observed, and its contribution to the output results was

Table 3 Flow rate and stable water level of production and reinjection wells

Water level in reinjection well (m)	Water level in production well (m)	Water level difference of production and reinjection well (m)	Flow rate (m^3/h)
5.94	3.53	2.41	1.10
5.61	3.72	1.89	0.72
5.38	4.19	1.19	0.52

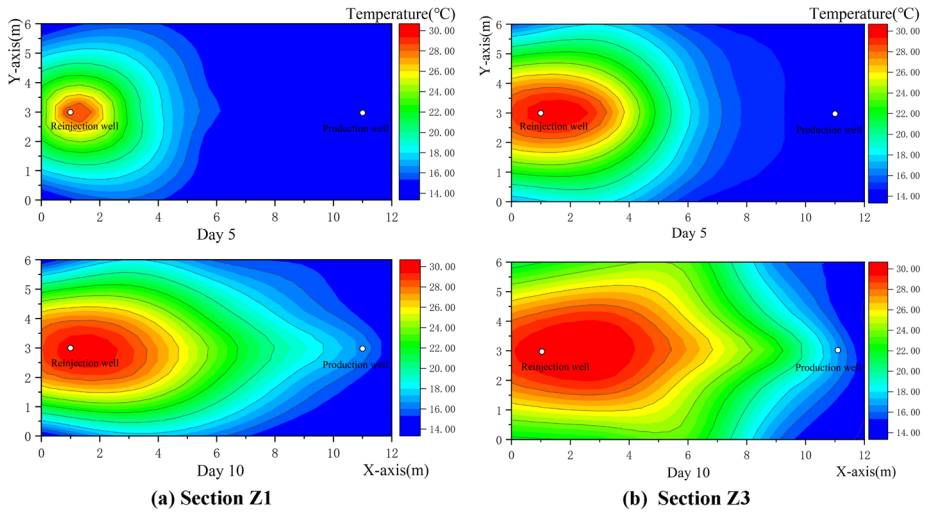

Fig. 7 Temperature cloud diagrams of the sand tank for a reinjection temperature of 30 °C

investigated. The sensitivity analysis of the reinjection parameters, including reinjection temperature and spacing between the production and reinjection wells, was carried out using the same approach.

Results

Experimental results of sand tank simulation model

Results of reinjection tests

After the reinjection tests were conducted using the sand tank simulation model with three stages (large drop depth, medium drop depth, and small drop depth), the different stable water levels in the production well corresponding to different production well flow rates were obtained (Table 3).

Results of heating reinjection tests

For a reinjection fluid temperature of 30 °C, all of the monitoring points in Sects. "Introduction" and "Results" in the *Z*-direction of the sand tank simulation test model (green and red monitoring surfaces in Fig. 5, respectively) were selected, and temperature clouds were plotted for the 5th and 10th days of reinjection (Fig. 7). The high-temperature fluid injected into the reinjection well gradually moved to the production well, and the temperature at each monitoring point along the X-axis increased gradually. At

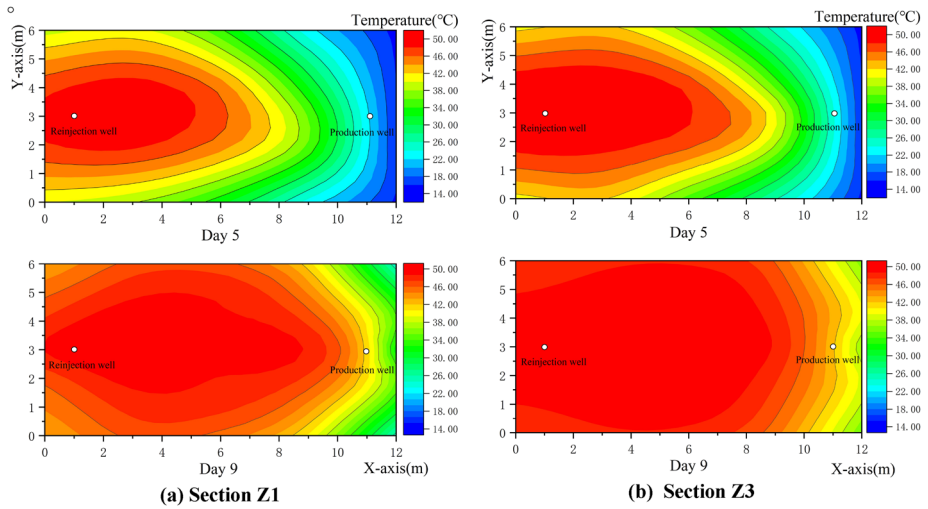

Fig. 8 Temperature cloud diagrams of the sand tank for a reinjection temperature of 50 °C

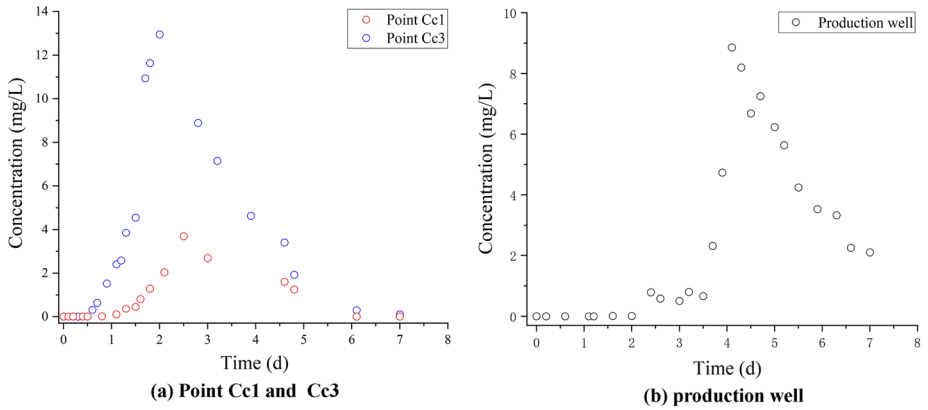

Fig. 9 Change in ammonium molybdate concentration in tracer tests

10 days, the Z3 cross section shows that the influence of the high-temperature fluid injected into the reinjection well reached the production well. Due to the difference in the permeability of the sand layer, the transport rate of the high-temperature fluid in the Z1 section was significantly lower than that in the Z3 section.

The temperature clouds for the 5th and 9th days for all of the monitoring points in cross-sections Z1 and Z3 were similarly plotted for a reinjection fluid temperature of 50 °C (Fig. 8). The high-temperature fluid injected in the reinjection well gradually moved toward the production well, but the rate of the fluid movement toward the production well and the temperature increase at the monitoring points increased significantly due to the increases in the reinjection temperature and reinjection rate. By day 5, the influence of the high-temperature fluids in cross-sections Z1 and Z3 had reached the production well. By day 10, the injected high-temperature fluids had basically filled the entire coarse sand layer where cross-section Z3 was located. Due to the difference in the permeability of the sand layer, the range of the high-temperature area in cross-section Z1 was still smaller than that in cross-section Z3.

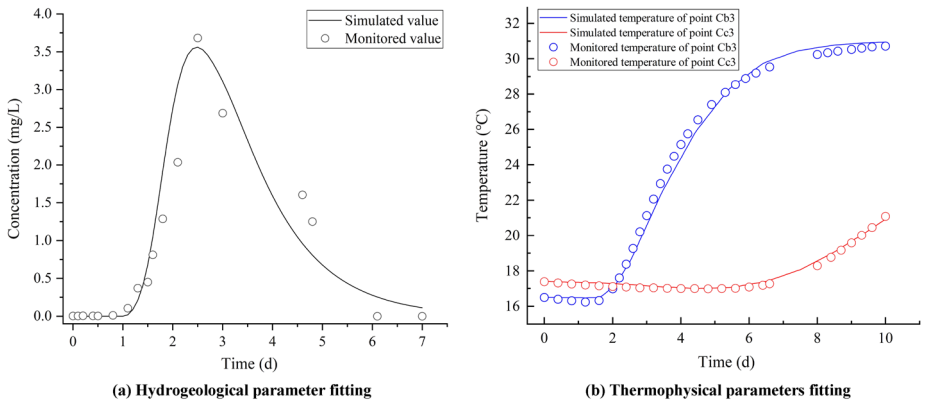

Fig. 10 Fitting curve of parameter

Table 4 Parameter values for numerical model of sand tank

Parameter	Unit	Value
Porosity		
Medium sand layer	–	0.25
Coarse sand layer	–	0.35
Permeability		
Medium sand layer	m^2	3×10^{-12}
Coarse sand layer	m^2	5.5×10^{-12}
Sand thermal conductivity	W/(m K)	2.4
Sand volumetric heat capacity	J/(K m^3)	2,100,000
Dispersion degree		
Medium sand layer	m	0.2
Coarse sand layer	m	0.5
Water thermal conductivity	W/(m K)	0.65
Water density	kg/m^3	998

Results of tracer tests

Two water sampling points (Cc1 and Cc3) inside the sand tank simulation test model were selected (their specific positions are shown in Fig. 6). The results are shown in Fig. 9. The ammonium molybdate reached point Cc1 after 0.7 days, and the concentration peaked at 2.5 days. The ammonium molybdate reached point Cc3 after 0.5 days, and the concentration peaked at 2 days. The ammonium molybdate reached production well after 2.5 days, and the concentration peaked at 4 and 4.6 days, respectively. After reaching the peak, the concentration gradually decreased. Due to the difference in the sand permeability, the arrival and peak times of the tracer at point Cc3 were sooner than those at point Cc1, and the peak concentration was also significantly higher than that at point Cc1.

Results of numerical simulation

Parameters of equivalent sand tank numerical model

When building an equivalent numerical model, the selection of the hydrogeological parameters is very important, and permeability is one of these important parameters. The magnitude of the permeability depends on the aquifer media. Since the water

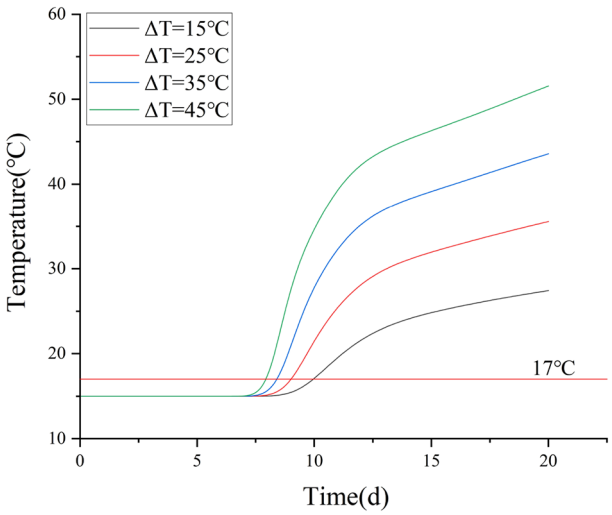

Fig. 11 Water temperature variations in production well for different reinjection temperature differences

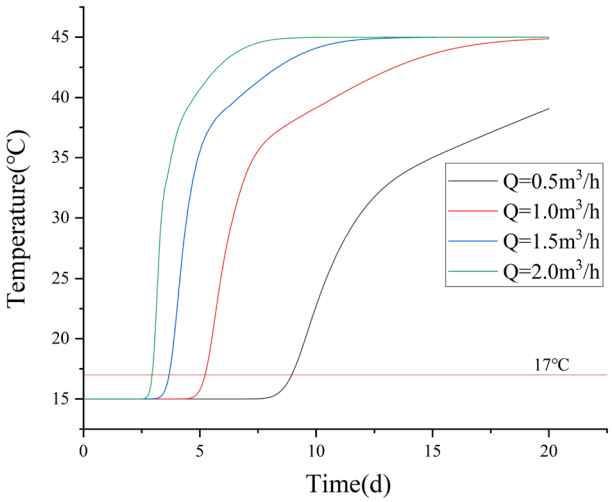

Fig. 12 Water temperature variations in production well for different reinjection rates

barrier was located 1 m outside the production and reinjection wells, the Dupuit and Theis formulas (Bear and Bachmat 1987; Theis 1935) for pressurized water wells were not applicable for obtaining the hydrogeological parameters of the simulation test model (e.g., the permeability coefficient, radius of influence, and unit surge volume). Therefore, the monitoring data from the reinjection tests, heating reinjection tests, and tracer tests were used to fit the hydrogeological parameters and thermal physical parameters of the sand tank model. The fitting effect is shown in Fig. 10 and the fitting results are presented in Table 4.

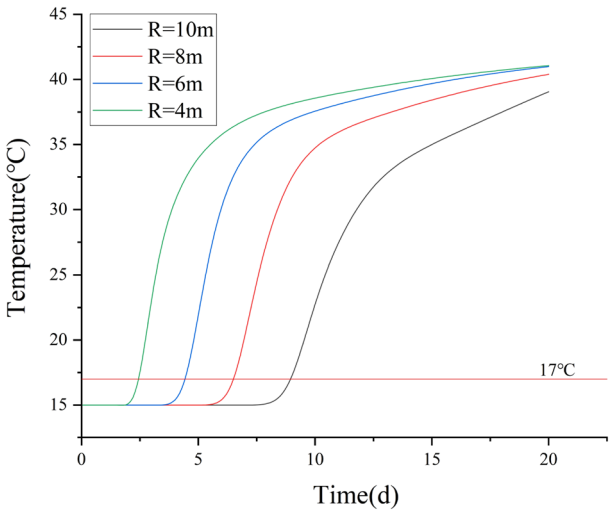

Fig. 13 Variations in water temperature in production well for different spacings between the production and reinjection wells

Relationships between reinjection parameters and water temperature variations in production well

To study the influences of the different reinjection parameters on the water temperature variations in the production well, the equivalent sand tank numerical model was used to calculate the water temperature variations in the production well under different reinjection temperatures, reinjection rates, and spacings between the production and reinjection wells, and the corresponding relationship curves were plotted (Figs. 11, 12, and 13, respectively). The temperature difference ΔT between production and reinjection is defined as the reinjection temperature minus the initial reservoir temperature.

The variations in the water temperature in the production well with time under different temperature difference ΔT between production and reinjection are shown in Fig. 11. The change trend of the water temperature in the production well under different reinjection temperature differences was basically the same. The temperature of the production water increased rapidly after the high-temperature geothermal water reached the production well, and then the temperature increase slowed down and gradually converged to the temperature of the reinjection water. The thermal breakthrough time t of the production well decreased as the temperature difference ΔT between production and reinjection increased. The variations in the water temperature with time in the production well under different reinjection rates Q are shown in Fig. 12. The trend of the water temperature in the production well was the same as that shown in Fig. 10, and the thermal breakthrough time t of the production well also decreased as the reinjection rate Q increased. The variations in the water temperature in the production well with time for different production and reinjection well spacings R are shown in Fig. 13. The variation trend of the water temperature of production well was still similar to that shown in Fig. 10, and the thermal breakthrough time t of the production well increased as the spacing R between the production and reinjection wells increased.

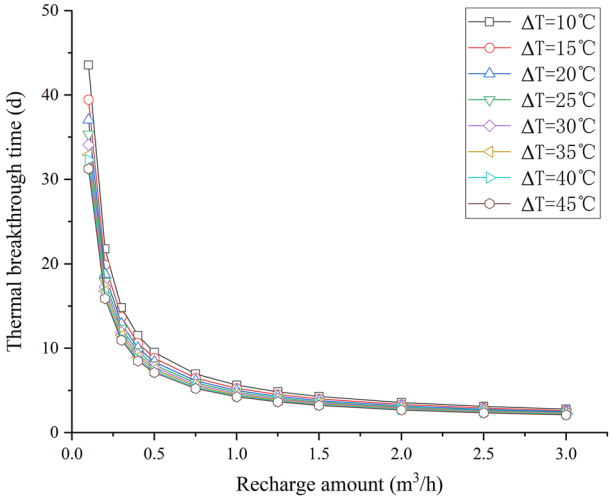

Fig. 14 Relationship between reinjection rate and thermal breakthrough time

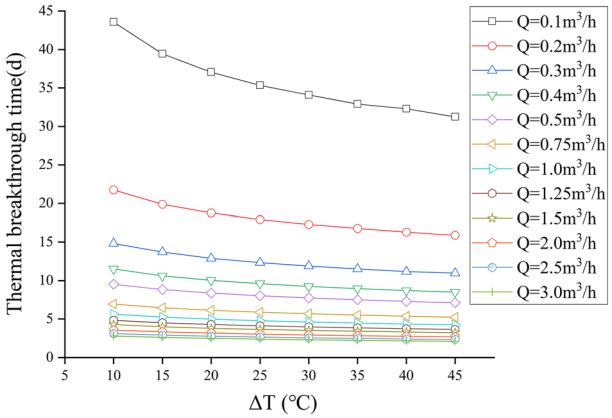

Fig. 15 Relationship between temperature difference between production and reinjection and thermal breakthrough time

Relationships between reinjection rate, reinjection temperature difference, and thermal breakthrough time

To study the influences of the reinjection temperature and reinjection rate on the thermal breakthrough time, the equivalent sand tank numerical model was used to calculate the thermal breakthrough time of the production well under different reinjection temperatures and reinjection rates, and the relationship between the reinjection rate and thermal breakthrough time and the relationship between the temperature difference ΔT between production and reinjection and thermal breakthrough time were plotted (Figs. 14, 15, respectively). As the reinjection rate Q and temperature difference ΔT between production and reinjection increased, the thermal breakthrough time of the production well decreased gradually, but it decreased more rapidly with increasing reinjection rate Q.

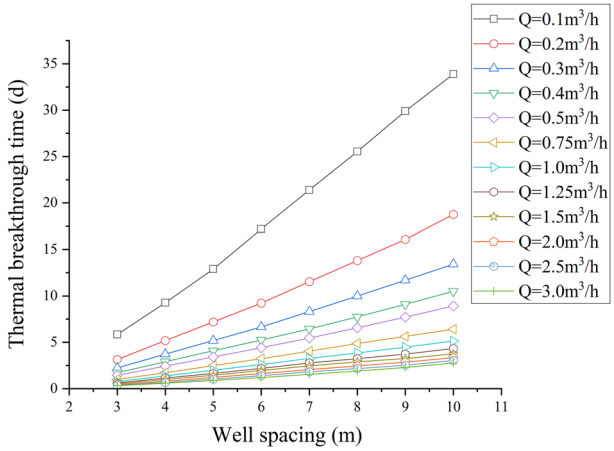

Fig. 16 Relationship between production and reinjection well spacing and thermal breakthrough time

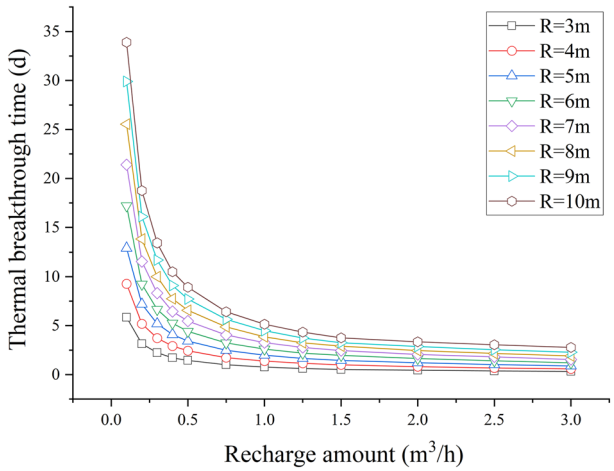

Fig. 17 Relationship between reinjection rate and thermal breakthrough time

Relationships between production and reinjection well spacing, reinjection rate, and thermal breakthrough time

Based on the average reinjection temperature of the actual project, the temperature difference ΔT between production and reinjection was set to 30 °C. Using the equivalent sand tank numerical model, the thermal breakthrough time of the production well was calculated under different reinjection rates and production and reinjection well spacings, and the relationships between the production and reinjection well spacing, reinjection rate, and thermal breakthrough time were plotted (Figs. 16, 17). The thermal breakthrough time of the production well decreased rapidly as the spacing R increased.

Parameter sensitivity analysis

To determine the response process and mechanism of the sandstone thermal reservoir temperature field to the reinjection parameters and to estimate the service life of the geothermal-to-well production and reinjection system, sensitivity analysis of three

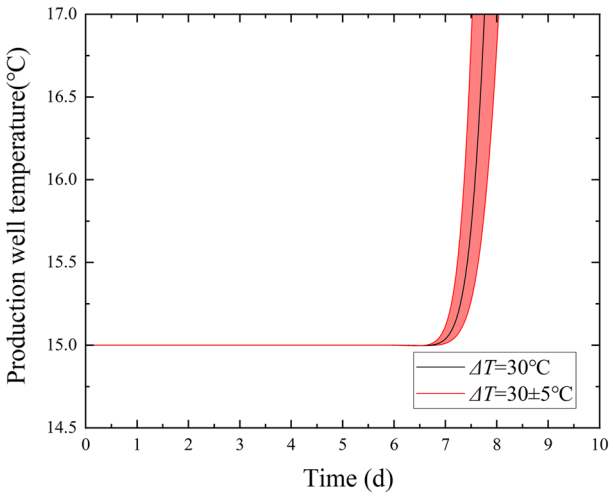

Fig. 18 Sensitivity of production well temperature to temperature difference between production and reinjection

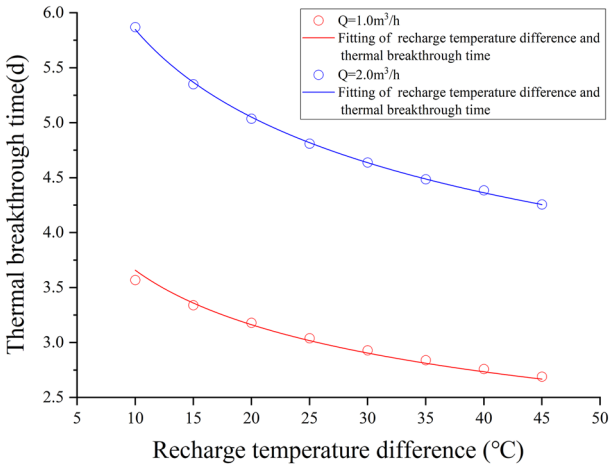

Fig. 19 Fitting of the relationship between the temperature difference between production and reinjection and the thermal breakthrough time

reinjection parameters (the reinjection temperature, reinjection rate, and production and reinjection well spacing) was conducted to determine the degrees of influence of the reinjection parameters on the thermal breakthrough time of the production well.

Temperature difference *ΔT* between production and reinjection

The fluid temperature of the reinjection water represents the heat returned to the reservoir. The temperature variation model of the production well was calculated for eight different reinjection rates for temperature difference ΔT between production and reinjection ΔT of 25 °C, 30 °C,. ..., and 60 °C and a production and reinjection well spacing of 10 m (Fig. 15). As the reinjection temperature increased, the thermal breakthrough time of the production well increased; however, as the reinjection

temperature continued to increase, its effect on the thermal breakthrough time of the production well rapidly decreased. When the reinjection temperature varied up and down by 5 °C from 30 °C, the temperature change before thermal breakthrough of the production well is shown in Fig. 18. The time when the water temperature of the production well started to decrease basically did not change as the reinjection temperature changed. The reinjection temperature fluctuated up and down by 16.7% from 30 °C, and the degree of influence on the thermal breakthrough time of the production well was within 6.9%. The results are shown in Fig. 19 and Eqs. (8) and (9). The thermal breakthrough time t of the production well was linearly correlated with $\Delta T^{-0.21}$, and the coefficient of linear relationship between t and $\Delta T^{-0.21}$ decreased with increasing Q:

$$t_{Q0.5} = 9.36\Delta T^{-0.21}, \tag{8}$$

$$t_{Q2.0} = 5.93\Delta T^{-0.21} \tag{9}$$

where t is the thermal breakthrough time of the production well [day]; subscripts Q 0.5 and Q2.0 indicate reinjection rate of 0.5 m^3/h and 2.0 m^3/h, respectively; and ΔT is the reinjection temperature difference [°C].

Spacing *R* between production and reinjection wells

Placing the production and reinjection wells at optimal distances from each other can significantly improve reservoir utilization. Increasing the well spacing can provide a greater range of recoverable reservoirs and therefore a longer service life. However, as the well spacing increases, the recovery rate of the system decreases. A smaller well spacing reduces the extent of the recoverable reservoir, resulting in a shorter system life, but most of the reinjection fluid can be recovered.

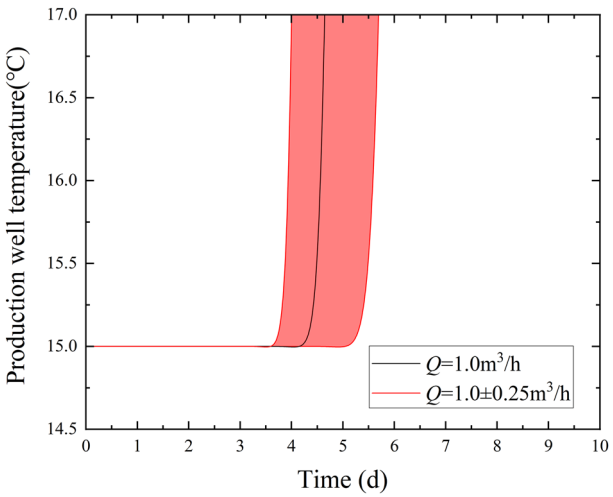

Fig. 20 Sensitivity of production well temperature to the spacing between the production and reinjection wells

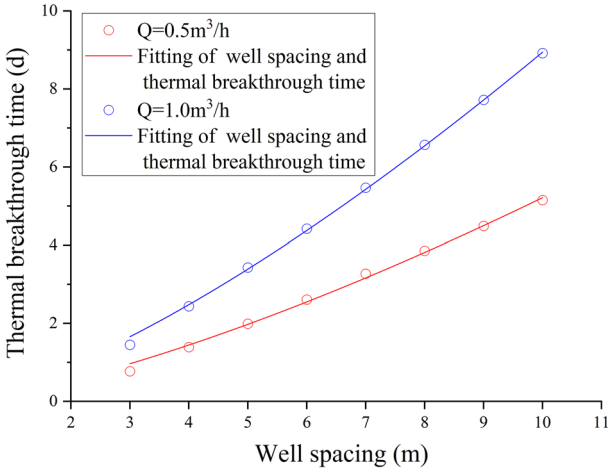

Fig. 21 Fitting of the relationship between the production and reinjection well spacing and the thermal breakthrough time

To quantitatively analyze the degree of influence of the spacing R between the production and reinjection wells on the thermal breakthrough time t of the production well, the temperature variations in the production well were studied under eight different production rates, eight different well spacings R of 3 m, 4 m,. … and 10 m, and the reinjection temperature difference of 30 °C (Fig. 16). As the production and reinjection well spacing R increased, both the thermal breakthrough time t and the rate of increase of the thermal breakthrough time t increased. When the production and reinjection rate was $Q = 1$ m^3/h, the production and reinjection well spacing R changed by 1 m up and down with 9 m as the center. The temperature change before the thermal breakthrough of the production well is shown in Fig. 20. The time when the water temperature in the production well started to decrease changed with the production and reinjection well spacing R. The spacing R between the production and reinjection wells fluctuated up and down by 11.1% from 9 m, and the degree of influence on the thermal breakthrough time of the production well reached 20.1%, which was much larger than the influence of the reinjection temperature difference ΔT. The results are shown in Fig. 21 and Eqs. (10) and (11). The thermal breakthrough time t of the production well was linearly correlated with the spacing $R^{1.4}$, and the coefficient of the linear relationship decreased as Q increased, which is the same as the coefficient in Eqs. (6) and (7):

$$t_{Q0.5} = 0.36R^{1.4}, \tag{10}$$

$$t_{Q1.0} = 0.21R^{1.4}, \tag{11}$$

where t is the thermal breakthrough time of the production well [day]; subscripts Q 0.5 and Q1.0 indicate reinjection rate of 0.5 m^3/h and 1.0m^3/h, respectively, and R is the production and reinjection well spacing [m].

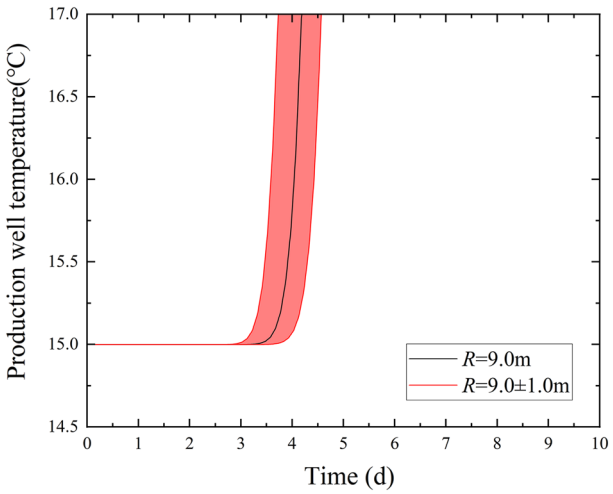

Fig. 22 Sensitivity of well temperature to reinjection rate

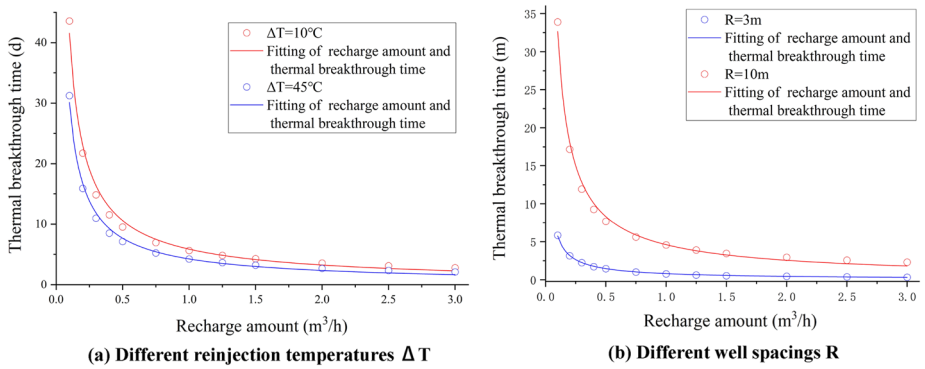

Fig. 23 Fitting of the relationship between the reinjection rate and the thermal breakthrough time

Reinjection rate *Q*

The reinjection rate is a parameter that can be adjusted after the operation of a geothermal-to-well production and reinjection system. It can have a direct impact on the system's lifetime and is one of the most important factors affecting the system's lifetime. To quantify the parameter sensitivity of the reinjection rate, a total of 12 cases were studied: 0.1 m^3/h, 0.2 m^3/h,. ....., 0.5 m^3/h, 0.75 m^3/h,. ....., 1.5 m^3/h, 2 m^3/h, 2.5 m^3/h, 2.5 m^3/h, and 3 m^3/h (Figs. 14, 17). As the reinjection rate Q increased, the thermal breakthrough time of the production well decreased rapidly. Compared with the results shown in Fig. 15, the effect of the reinjection rate Q on the thermal breakthrough time of the production well was significantly greater than that of the temperature difference ΔT between production and reinjection. When the well spacing was 10 m and the reinjection temperature difference was 30 °C, the reinjection rate Q varied up and down by 0.25 m^3/h with 1.0 m^3/h as the center. The temperature change before the thermal breakthrough of the production well is shown in Fig. 22. The time when the water temperature of the production well started to decrease varied greatly with the reinjection rate Q. The reinjection rate Q fluctuated up and down by 25.0% from 1.0 m^3/h, and the degree of influence on the thermal breakthrough

time of the production well reached 36.6%, which was much greater than the influence of the reinjection temperature difference ΔT. A well spacing of 10 m and reinjection temperature differences of 10 °C and 45 °C were selected to fit the relationship between the reinjection rate and the thermal breakthrough time of the production well. The results are shown in Fig. 23a and Eqs. (12) and (13). The thermal breakthrough time t of the production well was linearly correlated with $Q^{-0.85}$, and the coefficient of the linear relationship between t and $Q^{-0.85}$ decreased as the reinjection temperature difference ΔT increased, but the decrease was small, which is consistent with the results of the sensitivity analysis of ΔT. The results of the fitting of the reinjection rate and the thermal breakthrough time of the production well when the reinjection temperature difference was 30 °C and the production and reinjection well spacings were 3 m and 10 m are shown in Fig. 23b and Eqs. (14) and (15). When the well spacing R changed, the thermal breakthrough time of the production well t was still linearly correlated with $Q^{-0.85}$, which proves the reasonableness of the linear relationship between t and Q:

$$t_{10} = 5.87Q^{-0.85}, \tag{12}$$

$$t_{45} = 4.26Q^{-0.85}, \tag{13}$$

$$t_{R3} = 1.85Q^{-0.85}, \tag{14}$$

$$t_{R10} = 4.83Q^{-0.85}, \tag{15}$$

where t is the thermal breakthrough time of the production well [day]; subscripts 10 and 45 indicate that the temperature difference between production and reinjection is 10 ℃ and 45 ℃, respectively; subscripts $R3$ and $R10$ indicate that the spacing between production and reinjection wells is 3 m and 10 m, respectively, and Q is the reinjection rate [m^3/h].

Discussion

Effect of viscosity and density

To overcome the difficulty of heating the sand tank simulation model and the heat loss at boundary during the experiment, high-temperature reinjection was used to study the variations in water temperature and thermal breakthrough time of production well. The findings of the research may be affected by the reverse process wherein high-temperature fluid flows into low-temperature fluid, which counteracts the effect of low-temperature

Table 5 Parameter values of high-temperature and low-temperature reinjections

High-temperature reinjection	Initial temperature	15 ℃	15 ℃	15 ℃	15 ℃
	Injection temperature	25℃	35 ℃	45 ℃	55 ℃
Low-temperature reinjection	Initial temperature	25℃	35 ℃	45 ℃	55 ℃
	Injection temperature	15℃	15 ℃	15 ℃	15 ℃
Temperature difference ΔT		ΔT = 10℃	ΔT = 20 ℃	ΔT = 30 ℃	ΔT = 40 ℃

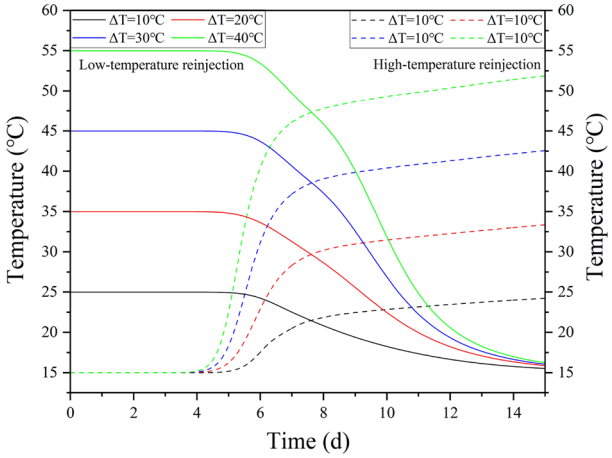

Fig. 24 Temperature variation curves of production well with high-temperature and low-temperature reinjection under different temperature differences between production and reinjection

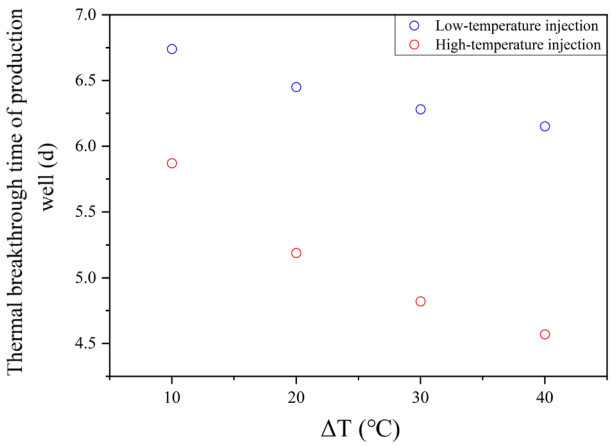

Fig. 25 Scatter diagram of thermal breakthrough time of production well with high-temperature and low-temperature reinjection under different temperature differences between production and reinjection

fluid flowing into high-temperature fluid. Moreover, variations in fluid temperature can lead to changes in viscosity and density, further influencing the research outcomes. In this study, we examined the influence of high-temperature reinjection and low-temperature reinjection on the research outcomes by varying the temperature difference ΔT between reinjection and production at 10 ℃, 20 ℃, 30 ℃, and 40 ℃.The parameters for reinjection are presented in Table 5.

In our investigation, the fluid density (ρ) was held constant at 1000 kg/m^3, while the fluid dynamic viscosity (μ) was varied according to temperature (as described by Eq. 16). We explored the impact of fluid viscosity on temperature variations and the thermal breakthrough time of the production well during high-temperature reinjection and low-temperature reinjection. The outcomes are presented in Figs. 24 and 25. It was observed that the temperature variations in the production well exhibited contrasting trends between high-temperature reinjection and low-temperature reinjection. Specifically, the temperature exhibited a higher rate of increase during high-temperature reinjection,

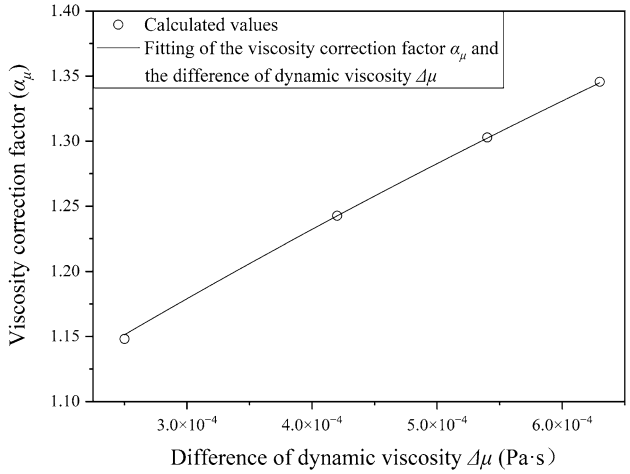

Fig. 26 Fitting of the relationship between the viscosity correction factor α_μ and the difference of dynamic viscosity $\Delta\mu$ of production and reinjection

while it decreased at a lower rate during low-temperature reinjection. Furthermore, for the same ΔT, the thermal breakthrough time during low-temperature reinjection was found to be longer compared to that during high-temperature reinjection.

With the increase in ΔT, the disparity in dynamic viscosity between the fluid in the sand tank simulation model and the reinjection fluid also increased. This led to a growing discrepancy when simulating the reverse process of low-temperature fluid migrating to high-temperature fluid using high-temperature fluid migrating to low-temperature fluid. To address this issue, we introduced a viscosity correction factor α_μ, which represents the ratio of the thermal breakthrough time of the production well during low-temperature reinjection to that during high-temperature reinjection. This factor was fitted against the difference in dynamic viscosity, $\Delta\mu$, corresponding to different ΔT. The relationship is illustrated in Fig. 26 and expressed by Eq. (17). The ratio α_μ, representing the thermal breakthrough time of the production well during low-temperature reinjection versus high-temperature reinjection, follows a logarithmic function of the dynamic viscosity difference $\Delta\mu$ between the sand tank water and the reinjection water.

$$\mu = 1.38 - 0.021T + 1.36 \times 10^{-4}T^2 (273.15K < T < 413.15K), \tag{16}$$

where μ is the dynamic viscosity of water and [Pa s]; T is the temperature of water [℃].

$$\alpha_\mu = \ln\left(1.78 \times 10^3 \Delta\mu + e\right), \tag{17}$$

where α_μ is the viscosity correction factor (the ratio of thermal breakthrough time of production well during low-temperature reinjection and high-temperature reinjection); $\Delta\mu$ is the dynamic viscosity difference between the sand tank water and the reinjection water with different temperatures [Pa s].

Under fixed parameters such as fluid dynamic viscosity (μ), an exploration was conducted to analyze the impact of high-temperature reinjection and low-temperature reinjection on temperature variations and the thermal breakthrough time of the production well, while considering the variation in fluid density (ρ) with temperature. The

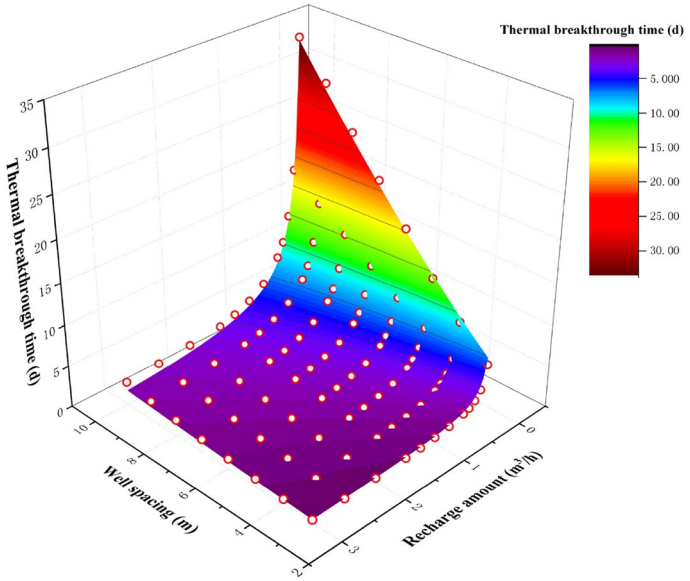

Fig. 27 Relationships between the thermal breakthrough time and the production and reinjection well spacing and reinjection rate

findings revealed that the influence of fluid density (ρ) on thermal breakthrough time was negligible, accounting for less than 5% when compared to the effect of dynamic viscosity (μ). Consequently, it can be inferred that errors may arise if low-temperature reinjection is replaced with high-temperature reinjection. This error primarily stems from fluctuations in fluid viscosity due to temperature changes, which can be rectified by introducing a viscosity correction coefficient (α_μ).

Therefore, for a constant reinjection temperature difference of 30 °C constant, nonlinear surface fitting of the change in the thermal breakthrough time t with the reinjection flow rate Q and the production and reinjection well spacing R was performed. The results are shown in Fig. 27 and Eq. (11). In the design of a geothermal-to-well production and reinjection system, a reasonable combination of reinjection flow rate Q and well spacing R can be determined according to the designed service life to ensure that no thermal breakthrough will occur in the production well during the designed service life. Considering the differences between model experiments and the actual reservoir parameters, the coefficients in Eq. (18) should be adjusted according to the parameters of the actual geothermal reservoir when used in practical applications.

$$t = 0.19\alpha_\mu R^{1.4} Q^{-0.85}, \tag{18}$$

Influence mechanism of reinjection parameters on geothermal reservoir temperature field

The inherent parameters of the thermal reservoir, such as the porosity and initial temperature, may have a large impact on the geothermal-to-well production and reinjection system, but these parameters are not artificially alterable. The reinjection rate, reinjection temperature, and production and reinjection well spacing are important artificially controlled parameters that can be optimized to obtain the longest service life and

highest energy productivity. The analysis results show that increasing the temperature difference ΔT between production and reinjection and reinjection rate Q will accelerate the thermal breakthrough time t of the production well, and increasing the production well spacing R will delay the thermal breakthrough time of the production well. ΔT has a significant effect on the thermal breakthrough time t of the production well when its absolute value is small, and the extent of its effect on the thermal breakthrough time of the production well decreases rapidly as ΔT increases. When the ΔT increases to about 30 ℃, the effect of a 1 ℃ fluctuation in ΔT on the thermal breakthrough time of the production well has been reduced to about 1.4%, which is basically negligible. In contrast, reinjection rate Q and well spacing R have great influence on thermal breakthrough time t, which shows that the influence mechanism of different reinjection parameters on the geo-temperature in reservoir is different.

The inherent parameters of the thermal reservoir, such as porosity and initial temperature, can significantly impact the geothermal-to-well production and reinjection system. However, these parameters are not subject to artificial alteration. On the other hand, the reinjection rate, reinjection temperature, and production and reinjection well spacing

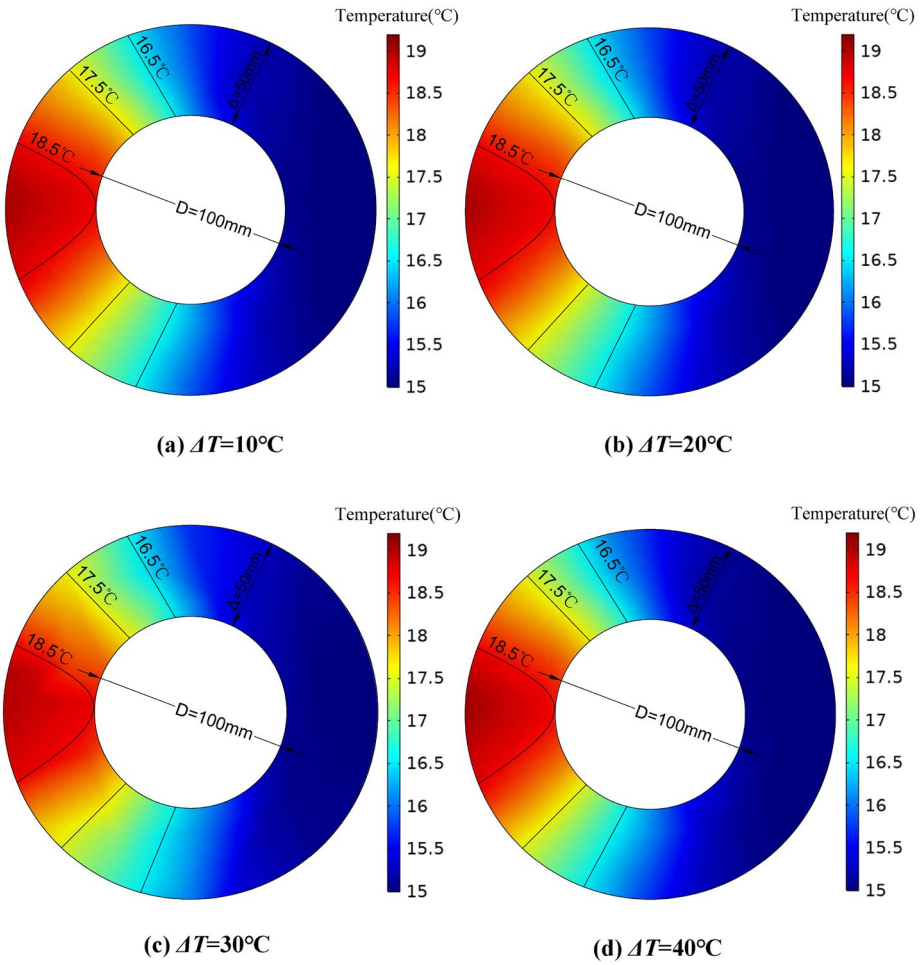

Fig. 28 Temperature graph of boreholes surrounding during thermal breakthrough in production well with different temperature difference ΔT

are important parameters that can be artificially controlled and optimized to enhance the system's service life and energy productivity. The analysis results indicate that an increase in the temperature difference (ΔT) between production and reinjection, as well as the reinjection rate (Q), accelerates the thermal breakthrough time (t) of the production well. Conversely, an increase in the production well spacing (R) delays the thermal breakthrough time. When ΔT is relatively small, it exerts a substantial impact on the thermal breakthrough time. However, this impact diminishes rapidly as ΔT increases. At about 30 ℃, a 1 ℃ fluctuation in ΔT only results in a negligible 1.4% variation in the thermal breakthrough time of the production well. In contrast, the reinjection rate (Q) and well spacing (R) exert a pronounced influence on the thermal breakthrough time (t). This indicates that different reinjection parameters have diverse influence mechanisms on the reservoir's geothermal temperature dynamics.

Figure 28 illustrates the microscopic temperature distribution within a 50 mm thickness around the wellbore when thermal breakthrough occurs in the production well. The analysis reveals that the temperature distribution near the wellbore remains relatively unchanged regardless of the temperature difference (ΔT) between production and reinjection. In the production well, thermal breakthrough occurs when the 18.5 ℃ isotherm front reaches the production shaft wall. Furthermore, Fig. 29 depicts the temperature

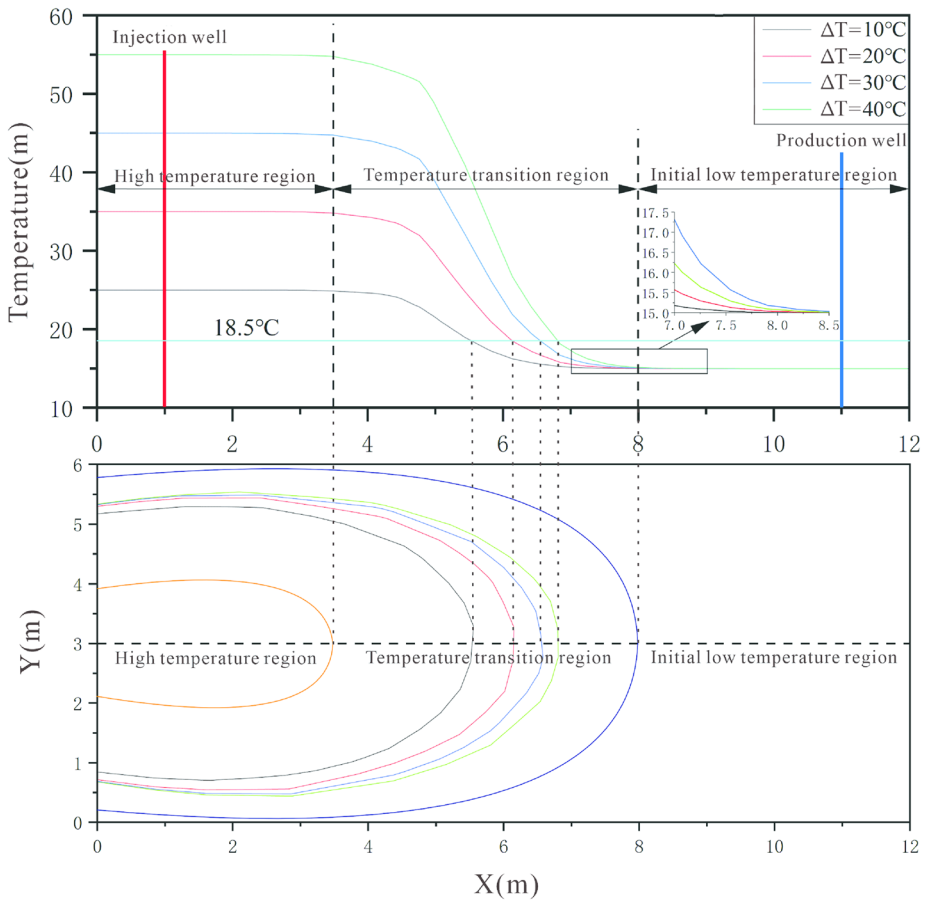

Fig. 29 Temperature distribution of central axis and plane of Z3 section at 2.5d with different temperature difference

distribution along the axis of the production and reinjection well, as well as the section Z, on the 2.5th day of reinjection at various temperature differences (ΔT). The geothermal temperature in the reservoir can be categorized into three regions: reinjection high-temperature region, initial low-temperature region, and temperature transition region. As ΔT increases, the width of the transition region expands slowly, with a decreasing growth rate. Specifically, when ΔT elevates from 30 ℃ to 40 ℃, the width of the transition region only increases by 2%. It can be inferred that when ΔT surpasses 30 ℃, the width of the temperature transition region tends to stabilize. Moreover, as ΔT continues to rise, only the temperature gradient in the transition region increases linearly. Consequently, the 18.5 ℃ isotherm within the temperature transition region gradually moves towards the front edge of the transition region due to the amplified temperature gradient, but the forward displacement attenuates. Hence, with an increasing ΔT, the time it takes for the 18.5 ℃ isotherm to reach the borehole wall advances, but the duration of advancement diminishes. This observation aligns with the consistent relationship between the temperature difference between production and reinjection and the thermal breakthrough time.

To summarize, the temperature discrepancy between reinjection water and the reservoir results in thermal conduction and convection at the interface of hot and cold water. This phenomenon creates a temperature transition region situated between the high-temperature reinjection area and the initial low-temperature region. The reinjection rate (Q) determines the rate at which reinjection water diffuses from the reinjection well into the surrounding area, consequently determining the overall displacement distance of the temperature transition region. Meanwhile, the spacing (R) between the production and reinjection wells determines the total migration distance of the temperature transition region towards the producing well. These two factors jointly dictate the timeframe required for the temperature transition region to reach the producing well. Furthermore, the temperature difference (ΔT) plays a role in determining the width of the transition region and the temperature gradient within it. These factors affect the breakthrough time (t) of the production well by influencing the relative position of the 18.5 °C isotherm line within the temperature transition region. The impact of ΔT on the thermal breakthrough time (t) depends on both the reinjection rate (Q) and the spacing (R), but its degree of influence is limited by these factors. Thus, as the absolute value of ΔT increases, the influence of ΔT on the thermal breakthrough time gradually decreases. In actual geothermal-to-well production and reinjection systems, the reinjection temperature difference (ΔT) is typically maintained above 30 °C. Therefore, the effect of ΔT on the thermal breakthrough time (t) of the production well is relatively weak and negligible when compared to the influences of the reinjection rate (Q) and production well spacing (R). Consequently, measures can be employed to reduce the reinjection temperature, thereby enhancing recovery efficiency and energy productivity in the reservoir.

Conclusions

In this study, the evolution of the internal temperature field of a thermal reservoir caused by reinjection was investigated through large sand tank simulation model tests and numerical simulations; the relationships between three reinjection parameters (i.e.,

the reinjection temperature, reinjection rate, and production and reinjection well spacing) and the thermal breakthrough time of the production well were quantitatively analyzed, and the influence of reinjection parameters on thermal breakthrough time of the production well and its internal mechanism and law are discussed. The main conclusions of this study are as follows:

1. The high-temperature fluid injected in the reinjection well gradually spread in all directions, causing the temperature field around the reinjection well to increase. After the hot water front reached the radius of the influence of the production well, the transport of the high-temperature fluid to the production well was accelerated and the hot water front extended toward the production well. Due to the difference in the permeability of the sand layers in the sand tank simulation test model, the evolution of the internal temperature field was different, and the transport rate of the high-temperature fluid in the upper medium sand layers was significantly smaller than that in the lower coarse sand layer.
2. After the high-temperature geothermal water reached the production well, the temperature of the production water increased rapidly, and then the temperature increase slowed down and gradually converged to the temperature of the reinjection water. The thermal breakthrough time (t) of the production well decreased as the reinjection flow rate (Q) and the reinjection temperature difference (ΔT) increased, and it increased as the production well spacing (R) increased.
3. The variations in the reinjection temperature difference (ΔT) had a significant effect on the thermal breakthrough time (t) of the production well when the absolute value was small, and the degree of its influence on the thermal breakthrough time (t) of the production wells decreased rapidly when it rises to more than 30 °C, suggesting that the recovery efficiency of heat reservoir can be improved by reducing the reinjection temperature. Compared with the reinjection temperature difference (ΔT), the variations in the reinjection rate (Q) and production and reinjection well spacing (R) always had greater influences on the thermal breakthrough time (t) of the production well, and the thermal breakthrough time (t) of the production well was linearly correlated with $Q^{-0.85}$, $\Delta T^{-0.21}$, and $R^{1.4}$.
4. The impact of reinjection from high-temperature fluid to low-temperature fluid, as opposed to the reverse flow, may introduce some inaccuracies primarily attributed to the temperature-dependent variation in fluid viscosity. To address this discrepancy, a viscosity correction coefficient, denoted as α_{μ}, can be utilized to rectify the error. This coefficient is characterized as a logarithmic function of the dynamic viscosity difference, $\Delta\mu$, between the sand tank water and the reinjection water.
5. The time it takes for the temperature transition region to reach the producing well is determined by the reinjection rate (Q) and the spacing (R). The width of the transition region and the temperature gradient within it are determined by the temperature difference (ΔT). The influence of ΔT on the thermal breakthrough time (t) is based on the interplay of the reinjection rate (Q) and the spacing (R). Thermal breakthrough occurs in the production well when the 18.5 °C isotherm front reaches the

wall of the production shaft. As ΔT increases, the 18.5 °C isotherm gradually moves towards the leading edge of the transition region, resulting in an advance in the time it takes for the 18.5 °C isotherm to reach the borehole wall. However, as the absolute value of ΔT increases, the advance in time caused by the elevation in ΔT gradually becomes shorter.

Acknowledgements
This research was financially supported by the National Natural Science Foundation of China (Grant Numbers 42072331, U1906209) and Taishan Scholar Foundation (No. tstp20230626). We are grateful to editors and reviewers for their constructive comments and valuable suggestions that significantly improved this manuscript.

Author contributions
JL completed sand tank simulation model test, numerical simulation, data analysis and paper writing. FK guided data analysis and paper writing. TB assisted in the sand tank simulation model test. ZL, QZ and PZ read and approved the final manuscript. TZ and HS guided the sand tank test program, and put forward valuable suggestions for the writing of the paper.

Funding
This research was financially supported by the National Natural Science Foundation of China (Grant Numbers 42072331, U1906209) and Taishan Scholar Foundation (No. tstp20230626).

Availability of data and materials
The datasets used and analyzed during the current study are available from the corresponding author on reasonable request.

Declarations

Competing interests
The authors declare that they have no competing interests.

Received: 21 August 2023 Accepted: 23 November 2023
Published online: 09 December 2023

References

Axelsson G, Gudmundsson A, Steingrimsson B, et al. Sustainable production of geothermal energy: suggested definition. IGA-News. 2001;43:1–2.
Axelsson G, Stefansson V, Xu Y. Sustainable management of geothermal resources. In: Proceedings of the International Symposium on Geothermal and the 2008 Olympics in Beijing, Beijing, China; 2002, pp. 277–283.
Axelsson G, Stefansson V, Björnsson G. Sustainable utilization of geothermal resources for 100–300 years. In Proceedings of the Twenty-Ninth Workshop on Geothermal Reservoir Engineering. Stanford University, California, United States; 2004, p. 10.
Axelsson G, Stefansson V, Björnsson G. Sustainable utilization of geothermal resources for 100–300 years. In: Proceedings of the World Geothermal Congress 2005, p. 8. Antalya, Turkey; 2005.
Ayling BF, Hogarth RA, Rose PE. Tracer testing at the Habanero EGS site, central Australia. Geothermics. 2016;63:15–26.
Bear J, Bachmat Y. Introduction to transport phenomena in porous media. Dordrecht: D. Rcidel Publishing Co; 1987.
Bedre MG, Anderson BJ. Sensitivity analysis of low-temperature geothermal reservoirs: effect of reservoir parameters on the direct use of geothermal energy. Trans Geotherm Resour Council. 2012;36:1255–61.
Bodvarsson G. Thermal problems in the siting of reinjection wells. Geothermics. 1972;1(2):63–6.
Cade CA, Evans IJ, Bryant SL. Analysis of permeability controls: a new approach. Clay Miner. 1994;29(4):491–501.
Chen M, Deng X, Wang J, Wang J. On the formation and accumulation of thermal water in North China Plain. Earth Sci. 1985;10(1):83–9.
Dutton SP, Loucks RG. Diagenetic controls on evolution of porosity and permeability in lower Tertiary Wilcox sandstones from shallow to ultradeep (200–6700 m) burial Gulf of Mexico Basin, USA. Mar Pet Geol. 2010;27(1):69–81.
Franco A, Vaccaro M. Numerical simulation of geothermal reservoirs for the sustainable design of energy plants: a review. Renew Sustain Energy Rev. 2014;30:987–1002.
Gao Z, Wu L, Li N, Cao H. Geothermal resources and their exploitation in Shandong Province. J Shandong Univ Sci Technol. 2009;28(2):1–7.
Guerrero FJ, Prol-Ledesma RM, Vidal-García MC, García-Zamorano EA, Hernández-Hernández MA, Pérez-Zárate D, Rodríguez-Díaz AA, Membrillo-Abad AS. A natural state model in TOUGH2 for the Las Tres Virgenes geothermal field, Baja California Sur, Mexico. Geothermics. 2023;113: 102750.

Hjuler ML, Olivarius M, Boldreel LO, et al. Multidisciplinary approach to assess geothermal potential, Tønder area, North German Basin. Geothermics. 2019;78:211–23.
Kang F. Sustainable yield and its assessment of geothermal reservoirs in China. Trans Geotherm Resour Council. 2013;37(4):843–52.
Kang F, Jin M, Qin P. Sustainable yield of a karst aquifer system: a case study of Jinan springs in northern China. Hydrogeol J. 2011;19(4):851–63.
Kang F, Zhang Z, Xu J, et al. Geothermal geological conditions and exploitation and utilization in Shandong Province. In: High Level Seminar Proceedings on Scientific Development of Chinese Geothermal Resources. pp. 79–83. Xianyang, China; 2013.
Lei HY, Zhu JL. Numerical simulation of pore type geothermal production and reinjection development scheme. Chin J Solar Energy. 2010;31(12):1633–8.
Liu ZT, Liu S, Song WH. Variation characteristics of geothermal tailwater reinjection in sandstone thermal reservoir in northern Shandong. Acta Geol Sin. 2019;2019(S1):149–56.
Liu G, Wang G, Zhao Z, et al. A new well pattern of cluster-layout for deep geothermal reservoirs: case study from the Dezhou geothermal field, China. Renewable Energy. 2020;155:1014–27.
McCreesh CA, Ehrlich R, Crabtree SJ. Petrography and reservoir physics II: relating thin section porosity to capillary pressure, the association between pore types and throat size 1. AAPG Bull. 1991;75:1563–78.
Megel T, Rybach L. Production capacity and sustainability of geothermal doublets. In Proceedings World Geothermal Congress. 2000; pp. 849–854. Kyushu-Tohoku, Japan.
Obembe AD, Abu-Khamsin SA, Hossain ME. A review of modeling thermal displacement processes in porous media. Arab J Sci Eng. 2016;41(12):4719–41.
O'Sullivan M, Mannington W. Renewability of the Wairakei-Tauhara geothermal resource. In: Proceedings of the World Geothermal Congress 2005; p. 8. Antalya, Turkey.
Qiu N, Xu W, Zuo Y, Chang J, Liu C. Evolution of Meso-Cenozoic thermal structure and thermal-rheological structure of the lithosphere in the Bohai Bay Basin, eastern North China Craton. Earth Sci Front. 2017;24(3):13–26.
Rybach L. Geothermal energy: sustainability and the environment. Geothermics. 2003;32(4–6):463–70.
Rybach L, Mégel T, Eugster WJ. How renewable are geothermal resources? Trans Geotherm Resour Council. 1999;23:563–6.
Saeid S, Al-Khoury R. A prototype design model for deep low-enthalpy hydrothermal systems. Renewable Energy. 2015;77:408–22.
Saeid S, Al-Khoury R, Nick HM. Experimental–numerical study of heat flow in deep low-enthalpy geothermal conditions. Renewable Energy. 2014;62:716–30.
Santoyo E, et al. Evaluation of artificial neural networks and eddy covariance measurements for modelling the CO_2 flux dynamics in the Acoculco geothermal caldera (Mexico). Int J Environ Sci Develop. 2018;9(10):298–302.
Sanyal SK. Sustainability and renewability of geothermal power capacity. In: Proceedings of the World Geothermal Congress 2005; p. 13. Antalya, Turkey.
Sauty JP, Gringarten AC, Landel PA. Lifetime optimization of low enthalpy geothermal doublets. In: Strub AS, Ungemach P, editors. Advances in European geothermal research. Berlin: Springer; 1980.
Sayantan G, Ganguly M. Analytical solutions for transient temperature distribution in a geothermal reservoir due to cold water reinjection. Hydrogeol J. 2014;22:351–69.
Seibt P, Kellner T. Practical experience in the reinjection of cooled thermal waters back into sandstone reservoirs. Geothermics. 2003;32(4–6):733–41.
Sippel J, Fuchs S, Cacace M. Deep 3D thermal modelling for the city of Berlin (Germany). Environ Earth Sci. 2013;70(8):3545–66.
Stefansson V. The renewability of geothermal energy. In: Proceedings of the World Geothermal Congress 2000; pp. 883–888. Kyushu-Tohoku, Japan.
Theis CV. The relation between the lowering of the Piezometric surface and the rate and duration of discharge of a well using ground-water storage. EOS Trans Am Geophys Union. 1935;16(2):519–24.
Tomasini-Montenegro C, Santoyo-Castelazo E, Gujba H, Romero RJ, Santoyo E. Life cycle assessment of geothermal power generation technologies: an updated review. Appl Therm Eng. 2017;114:1119–36.
Wang Y, Liu G, Hu S. Division of the geothermal resources in the northern Shandong Province. Geolog Survey Res. 2008;31(3):270–7.
Weibel R, Olivarius M, Kristensen L, et al. Predicting permeability of low-enthalpy geothermal reservoirs: a case study from the Upper Triassic—Lower Jurassic Gassum Formation, Norwegian-Danish Basin. Geothermics. 2017;65:135–57.
Wright PM. The sustainability of production from geothermal resources. In: Proceedings World Geothermal Congress 1995; pp. 2825–2836. Florence, Italy.
Wu LJ, Zhao JC, Li AY. Research on key issues of geothermal resources development and utilization in lubei depression. Geol Explor. 2016;52(2):300–6.
Zhao JC. Lubei geothermal tail water reinjection tests in sandstone reservoir. Shandong Land Resour. 2013;29:23–30.
Zhu JL, Zhu XM, Lei HY. Analysis of the influence of pressure difference compensation between geothermal reinjection wells on reinjection efficiency. J Solar Energy. 2012;033(001):56–62.

Jialong Li (1995), male, Ph.D. candidate, primarily engaged in geothermal resource exploration, exploitation, and reinjection research.

Fengxin Kang (1968), male, Professor, Ph.D., Taishan Scholar, primarily engaged in hydrogeology and geothermal geology research.